Ultrafast X-ray Scattering

DOI: 10.1002/ange.200801153

Ultrafast X-Ray Solution Scattering Reveals an Unknown Reaction Intermediate in the Photolysis of $[Ru_3(CO)_{12}]$**

Qingyu Kong, Jae Hyuk Lee, Anton Plech, Michael Wulff, Hyotcherl Ihee, and Michel H. J. Koch*

The triangular metal carbonyl cluster $[Ru_3(CO)_{12}]$, which is one of the simplest thermally stable metal carbonyls, has served as an example for the photochemistry of transition metal carbonyls. This complex is used in controlled photoactivated synthesis whereby specific types of bonds in the complex are broken at specific wavelengths.[1,2] As the mechanism leading to the cleavage of metal–metal bonds is of great theoretical and practical interest,[3,4] photolysis of $[Ru_3(CO)_{12}]$ has been extensively studied by spectroscopy in solid matrices and in solution.[2,5–12] With the exception of ultrafast infrared spectroscopy, which has been most efficient in identifying intermediates based on the detection of bridging CO ligands, most techniques have failed to characterize the structure of the intermediates. Recent ultrafast infrared spectroscopic measurements have shown that when solutions of $[Ru_3(CO)_{12}]$ in noncoordinating solvents like cyclohexane are excited with either an ultraviolet (266 nm) or a visible (400 nm) optical pulse, competing reactions yield two transient intermediates containing bridging carbonyl ligands: $[Ru_3(CO)_{11}(\mu\text{-CO})]$ (Intermediate 1) for the metal–metal cleavage reaction channel and $[Ru_3(CO)_{10}(\mu\text{-CO})]$ (Intermediate 2) for the CO-loss reaction channel.[12] Figure 1 a shows the molecular structures of the parent molecule, known Intermediates 1 and 2, and the newly identified intermediate (Intermediate 3) from this study. The subsequent reactions depend strongly on the properties of the solvent. In noncoordinating solvents like alkanes both intermediates relax to the parent molecule, whereas more complex fragmentation and complexation reactions occur in π-accepting solvents or in the presence of π-backbonding ligands such as CO. Infrared spectroscopy very specifically monitors the time course of the concentration of these two intermediates via the absorption bands of their bridging carbonyl ligands. This leaves the possibility that other intermediates, especially those containing only terminal carbonyl ligands with absorption bands that overlap with those of the parent molecule, would go unnoticed.

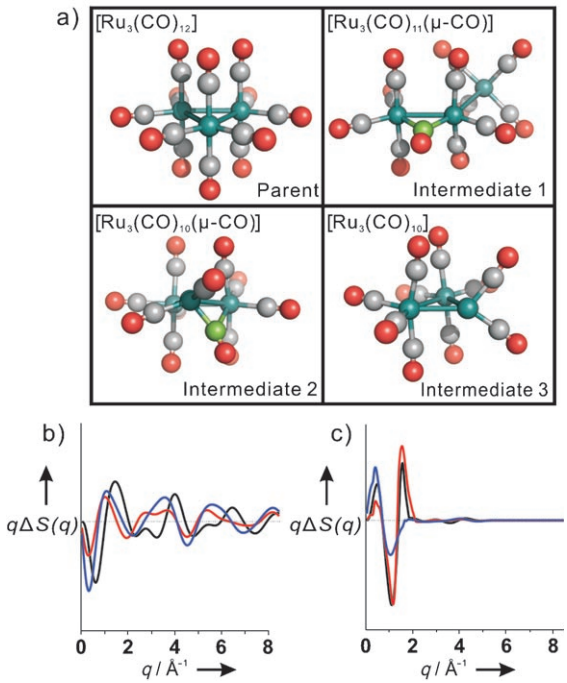

Figure 1. Molecular structures and their difference scattering intensities $q\Delta S(q)$. a) Molecular structures of $[Ru_3(CO)_{12}]$ and the principal species formed after photolysis in noncoordinating or σ-donating solvents. Ru, C, and O atoms are colored in cyan, gray, and red, respectively. To distinguish bridging carbonyl ligands, their carbon atoms are colored in green. Intermediates 1 and 2 were identified previously by ultrafast infrared spectroscopy based on the detection of bridging carbonyl ligands. The new Intermediate 3 is the major transient according to ultrafast X-ray scattering. b) Solute-only theoretical difference scattering curves for each intermediate formation channel (black: Intermediate 1, blue: Intermediate 2, red: Intermediate 3). The curves for other candidate species are shown in Figure S4. Each curve has characteristic oscillations and can therefore be used to fingerprint the reaction intermediate. c) Solute/solvent cross-term for each reaction channel. In contrast to the solute-only curves, the low-q signal dominates. Parts (b) and (c) are on the same scale.

[*] J. H. Lee, Prof. H. Ihee
Center for Time-Resolved Diffraction, Department of Chemistry (BK21), KAIST, Daejeon, 305-701 (Republic of Korea)
Fax: (+82) 42-869-2810
E-mail: hyotcherl.ihee@kaist.ac.kr
Homepage: http://time.kaist.ac.kr
Dr. Q. Kong, Prof. M. Wulff
European Synchrotron Radiation Facility
6 Rue Jules Horowitz, BP220, 38043 Grenoble Cedex (France)
Dr. A. Plech
Fachbereich Physik der Universität Konstanz
Universitätsstrasse 10, 78457 Konstanz (Germany)
Prof. M. H. J. Koch
European Molecular Biology Laboratory, Hamburg Outstation, EMBL c/o DESY, Notkestrasse 85, 22603 Hamburg (Germany)

[**] We thank Maciej Lorenc, Friederike Ewald, Marco Cammarata, Kyung Hwan Kim, Morten Christensen, and Savo Bratos for their help in the experiment and theory. This work was supported by EU grants FAMTO (HPRICT-1999-50004) and FLASH (FP6-503641) and by Creative Research Initiatives (Center for Time-Resolved Diffraction) of MOST/KOSEF awarded to H.I.

Supporting information for this article is available on the WWW under http://www.angewandte.org or from the author.

In contrast, the signal from time-resolved X-ray or electron scattering contains contributions from all interatomic distances in the volume probed by the incident beam.[13–16] As shown in Figure 1b, each intermediate species gives its own scattering pattern, which can therefore be used to follow the time course of its concentration. However, except for the simplest cases, there is no unique solution to recover the three-dimensional structural information from scattering data, and this inverse problem can only be solved by modeling based on theoretical calculations. The application of this method to the photodissociation of $[Ru_3(CO)_{12}]$ dissolved in cyclohexane at a wavelength of 390 nm clearly shows that the main photoproduct is one of the $[Ru_3(CO)_{10}]$ complex isomers (Intermediate 3) with a $\{Ru_3\}$ ring and only terminal carbonyl ligands, which has a lifetime of tens of nanoseconds. The other $[Ru_3(CO)_{10}]$ isomers with bridging carbonyl ligands do not match the time-resolved scattering data.

A pump–probe experiment was performed on beamline ID09B of the European Synchrotron Radiation Facility with femtosecond laser pulses (390 nm) for excitation and 100-picosecond X-ray pulses for probing the transient structures from the photolysis of $[Ru_3(CO)_{12}]$ in solution. The difference X-ray scattering intensities $q\Delta S(q,t)$ illustrating the structural changes due to the laser excitation are shown in Figure 2a as a function of the momentum transfer $q = 4\pi\sin\theta/\lambda$, where 2θ is the scattering angle and λ the average wavelength (0.69 Å) of the polychromatic incident X-ray beam with 3% bandwidth.[17] They were obtained by subtracting the pattern measured at −3 ns (i.e., before excitation) from all others in the time series, as described previously.[13–16] The experimental $q\Delta S(q,t)$ curves were globally fitted with theoretical difference scattering intensities containing three contributions associated with 1) the structural changes of the solute(s), 2) the changes in the solvation cage caused by solute/solvent interactions, and 3) the response of the bulk solvent to heating and thermal expansion.[14–16] The results of the fit are also shown in Figure 2a. Contribution 1 from the structural changes of the solutes is calculated from the difference between the Debye scattering curves of models of putative intermediates and the parent molecule obtained by DFT. The solute/solvent interaction (contribution 2) for each putative intermediate is calculated by molecular dynamics (MD) simulations with a single molecule in a solvent box of fixed size. The bulk solvent response (contribution 3) is deduced from the measured impulsive heating of the pure solvent excited by near-infrared laser photons.[18] The total theoretical curve is the sum of these three components, as shown in Figure 2b for the data at 100 ps. In fact, due to weak intermolecular forces between the cyclohexane solvent molecules, the high-q signal can be approximated as originating from naked solutes only.[13,14] For comparison with the experimental data the theoretical curves were convoluted with the wavelength profile of the X-ray beam (i.e., the incident beam after correction for absorption).

Initial attempts at fitting the curves with only the known Intermediates 1 and 2 did not give satisfactory results (Figure S6 in the Supporting Information) and suggested the presence of a third intermediate. As Intermediates 1 and 2 are known to have decay times on the order of 150 ps and 5 ns, respectively,[12] the signal from the new intermediate should dominate at longer times. To characterize the new intermediate, the experimental $q\Delta S(q,t)$ profile at 30 ns was compared with those of a series of candidate molecules. The reaction channel $[Ru_3(CO)_{12}] \rightarrow [Ru_3(CO)_{10}] + 2\,CO$ matches almost perfectly the experimental data over the entire q range (Figure 2c). $[Ru_3(CO)_{10}]$ has three isomers, but only one of them (Intermediate 3) has no bridging carbonyl ligands (Figure S2). Since the q region above 2.4 $Å^{-1}$ is dominated by the solute-only term, we fitted this region at 10 ns with the three candidate intermediates. Intermediate 3 gives the best agreement with the experiment (Figure S7). When the three intermediates are included in the fit, the concentrations of the other two intermediates converge to zero. This finding suggests that previous time-resolved infrared spectroscopic studies missed this $[Ru_3(CO)_{10}]$ intermediate due to the absence of any bridging carbonyl ligand. Then, to obtain the overall kinetics, the data from all time delays were fitted simultaneously by means of a global fitting analysis[14–16] by including the parent molecule, Intermedi-

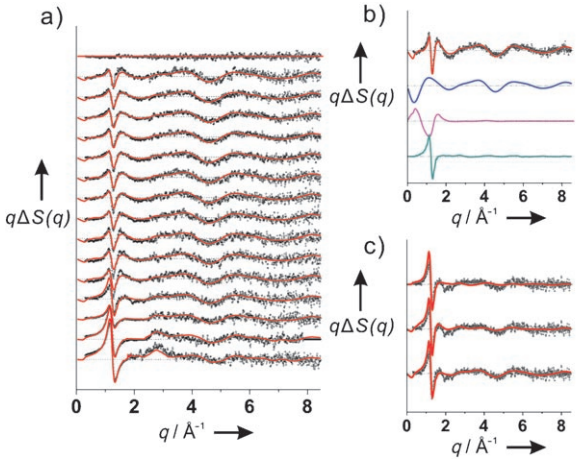

Figure 2. Experimental and theoretical difference scattering intensities $q\Delta S(q,t)$ and data analysis. a) Time-resolved difference scattering intensities $q\Delta S(q,t)$ as a function of time delay after photolysis of $[Ru_3(CO)_{12}]$ in cyclohexane. The black dots correspond to the experimental data and the red curves to the theoretical least-squares fits (global fitting analysis). The time delays from top to bottom are −100 ps, 42 ps, 60 ps, 75 ps, 100 ps, 200 ps, 300 ps, 500 ps, 1 ns, 3 ns, 5 ns, 10 ns, 30 ns, 50 ns, 100 ns, and 300 ns. The values in the low-q region of the first 13 curves and the last three curves have been divided by 3 and 6, respectively, for clarity. b) Time-resolved data at 100 ps. The theoretical model (red curve) has three contributions: the transient solute (blue), the solute/solvent interaction (magenta), and the response of the bulk solvent to thermal expansion and temperature change (green). The solute signal is calculated from the Debye scattering of the putative solutes, the solute/solvent interaction (cage) is calculated by MD simulation, and the solvent signal is deduced from impulsive heating of pure cyclohexane excited with a near-infrared pulse. c) Determination of the photoproducts at 30 ns and characterization of Intermediate 3. Experimental (black) and theoretical (red) difference scattering intensities $q\Delta S(q,t)$ for various candidate reaction channels (top: Intermediate 1, middle: Intermediate 2, and bottom: Intermediate 3) are shown. The channel for Intermediate 3 gives the best agreement between experiment and theory.

ate 2, and Intermediate 3 (Figure 2a). As illustrated in Figure 2a, the introduction of $[Ru_3(CO)_{10}]$ as a new intermediate in the global least-squares refinement considerably improves the fit, not only for longer time delays, but also for shorter times, that is, this intermediate is formed at the onset of the reaction. In addition, the fact that the curves at 42, 60, 75, and 100 ps are almost identical once normalized to the X-ray flux (see Supporting Information) indicates that all intermediates form within 42 ps. In terms of energy, one photon at 390 nm provides sufficient energy for the detachment of two CO ligands to produce Intermediate 3. Whether Intermediate 3 is formed directly from the excited parent molecule or sequentially via a $[Ru_3(CO)_{11}]$ species could not be established here.

Figure 3b shows the time course of the populations of the three intermediates and the parent molecule determined with

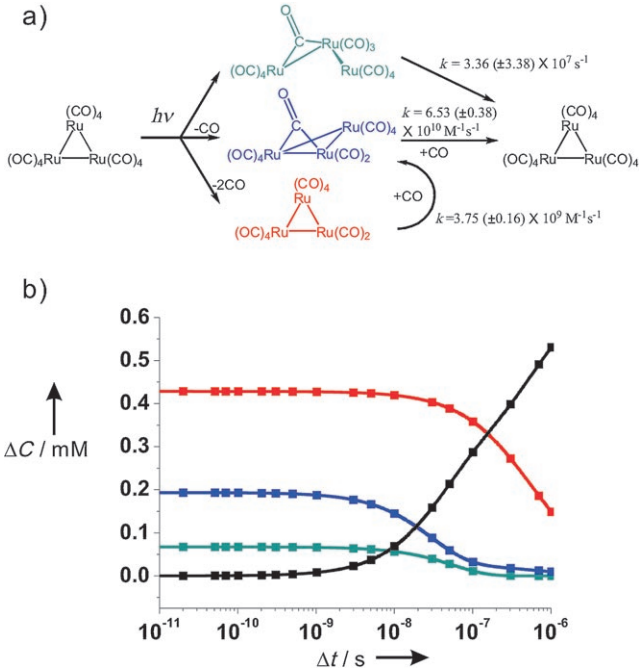

Figure 3. Reaction pathways and concentration changes. a) Photochemical reaction pathways of the photolysis of $[Ru_3(CO)_{12}]$ in cyclohexane and their associated rate constants determined in this study. Within the available time resolution, three intermediates form and return to the parent species. b) Concentration changes of the relevant chemical species during the photoreaction as a function of time (cyan: Intermediate 1, blue: Intermediate 2, red: Intermediate 3, black: parent molecule).

the fitted rate constants from the global fitting based on the schematic reaction mechanism (Figure 3a) used in this study. The concentrations obtained by time-resolved scattering depend to some extent on the choice of the fitting range and on the exact geometry of the models. Since the X-ray pulse width is 100 ps (full width at half-maximum) and the earliest time delay is 42 ps, our data is more sensitive to the decay time than to the rise time of the intermediates. Intermediate 1 presumably decays exponentially to the initial $[Ru_3(CO)_{12}]$ with a unimolecular rate constant of $(3.36 \pm 3.38) \times 10^7\ s^{-1}$. As it is a very minor species, the error associated with its decay time is rather large. In fact, a reasonably good fit can be obtained without including this intermediate. By contrast, the $[Ru_3(CO)_{10}(\mu\text{-}CO)]$ Intermediate 2 was necessary to obtain a reasonable fit. According to the result of the fit, it recombines nongeminately with a CO ligand to return to the parent molecule $[Ru_3(CO)_{12}]$ with a bimolecular rate constant of $(6.53 \pm 0.38) \times 10^{10}\ M^{-1}\ s^{-1}$. Intermediate 3 dominates at all time delays. It decays to Intermediate 2 with a bimolecular rate constant of $(3.75 \pm 0.16) \times 10^9\ M^{-1}\ s^{-1}$. Since the decay rate of Intermediate 3 is much slower than that of Intermediate 2, the latter does not accumulate from the decay of Intermediate 3. Hence, any intermediate with the formula $[Ru_3(CO)_{11}]$ is a candidate for the actual intermediate formed from nongeminate recombination of Intermediate 3 and CO. The exact structure of this intermediate connecting Intermediate 3 and the parent molecule could not be determined in this study. The simultaneous formation of binuclear $[Ru_2(CO)_9]$, $[Ru_2(CO)_8]$, or $[Ru_2(CO)_6]$ species by loss of one of the mononuclear units $\{Ru(CO)_3\}$, $\{Ru(CO)_4\}$, or $\{Ru(CO)_5\}$, although thermodynamically favored (Table S1), is not observed.

As the Ru–Ru distances contribute more than 90% of the coherent scattering signal, we attempted to optimize the initial DFT geometries of $[Ru_3(CO)_{12}]$ and the transient intermediates by refining a single scaling parameter applied to all Ru–Ru distances calculated by DFT. The optimized experimental bond lengths in Table 1 are shorter by a factor of 0.983 than those obtained by DFT, which is consistent with the general tendency of DFT to overestimate metal–metal distances.[19]

Table 1: Ru–Ru bond lengths [Å] obtained by least-squares refinement of the time-resolved X-ray scattering data and DFT calculations.

Species	Experiment[a,b]	DFT
$[Ru_3(CO)_{12}]$	Ru1–Ru2: 2.88	2.93
	Ru1–Ru3: 2.88	2.93
	Ru2–Ru3: 2.88	2.93
Intermediate 1, $[Ru_3(CO)_{11}(\mu\text{-}CO)]$	Ru1–Ru2: 2.86	2.91
	Ru1–Ru3: 5.05	5.14
	Ru2–Ru3: 3.12	3.17
Intermediate 2, $[Ru_3(CO)_{10}(\mu\text{-}CO)]$	Ru1–Ru2: 2.76	2.81
	Ru1–Ru3: 2.89	2.94
	Ru2–Ru3: 2.79	2.84
Intermediate 3, $[Ru_3(CO)_{10}]$	Ru1–Ru2: 2.66	2.71
	Ru1–Ru3: 2.89	2.94
	Ru2–Ru3: 2.68	2.73

[a] A single scale factor was refined and used to scale all DFT values. [b] The actual errors associated with the fits are smaller than the last digit.

The results reported here strikingly illustrate the complementary nature of ultrafast X-ray scattering[12–18,20–22] and ultrafast spectroscopy,[12] which will be a key factor in the successful use of advanced X-ray sources.[23] Indeed, a good fit to the experimental X-ray scattering data can only be obtained if Intermediate 3, which does not contain a bridging carbonyl ligand and is thus invisible to infrared spectroscopy, is included in the refinement. X-ray scattering alone, how-

ever, could not have established the existence of the minor intermediate $[Ru_3(CO)_{11}(\mu\text{-}CO)]$, because its contribution to the overall scattering curve is much smaller than that of $[Ru_3(CO)_{10}]$ (Figure S6). This would, however, contradict the spectroscopic results, which unequivocally establish the existence of two intermediates containing bridging carbonyl ligands.[12] In conclusion, the results of the two techniques clearly indicate the existence of at least three intermediates with very different molecular structures.

Experimental Section

$[Ru_3(CO)_{12}]$ (99%) (Sigma-Aldrich) and spectroscopic-grade cyclohexane (Sigma-Aldrich) (>99.5%) were used without further purification to prepare an approximately 3 mM solution, which was filtered before the measurements. The experimental setup of the ID09B beamline at the European Synchrotron Radiation Facility (ESRF) is described in detail elsewhere[13–16] and in the Supporting Information.

Received: March 10, 2008
Published online: June 20, 2008

Keywords: carbonyl ligands · photochemistry · reaction mechanisms · time-resolved spectroscopy · X-ray scattering

[1] J. G. Bentsen, M. S. Wrighton, *J. Am. Chem. Soc.* **1987**, *109*, 4530.
[2] B. F. G. Johnson, J. Lewis, M. V. Twigg, *J. Organomet. Chem.* **1974**, *67*, C75.
[3] M. G. Richmond, *Coord. Chem. Rev.* **2004**, *248*, 881.
[4] Y. M. Wuu, J. G. Bentsen, C. G. Brinkley, M. S. Wrighton, *Inorg. Chem.* **1987**, *26*, 530.
[5] J. G. Bentsen, M. S. Wrighton, *J. Am. Chem. Soc.* **1987**, *109*, 4518.
[6] M. F. Desrosiers, P. C. Ford, *Organometallics* **1982**, *1*, 1715.
[7] J. Malito, S. Markiewitz, A. Poe, *Inorg. Chem.* **1982**, *21*, 4335.
[8] J. L. Graff, R. D. Sanner, M. S. Wrighton, *J. Am. Chem. Soc.* **1979**, *101*, 273.
[9] F. W. Grevels, J. G. A. Reuvers, J. Takats, *J. Am. Chem. Soc.* **1981**, *103*, 4069.
[10] M. F. Desrosiers, D. A. Wink, R. Trautman, A. E. Friedman, P. C. Ford, *J. Am. Chem. Soc.* **1986**, *108*, 1917.
[11] F. W. Grevels, W. E. Klotzbucher, J. Schrickel, K. Schaffner, *J. Am. Chem. Soc.* **1994**, *116*, 6229.
[12] E. A. Glascoe, M. F. Kling, J. E. Shanoski, C. B. Harris, *Organometallics* **2006**, *25*, 775.
[13] A. Plech, M. Wulff, S. Bratos, F. Mirloup, R. Vuilleumier, F. Schotte, P. A. Anfinrud, *Phys. Rev. Lett.* **2004**, *92*, 125505.
[14] H. Ihee, M. Lorenc, T. K. Kim, Q. Y. Kong, M. Cammarata, J. H. Lee, S. Bratos, M. Wulff, *Science* **2005**, *309*, 1223.
[15] T. K. Kim, M. Lorenc, J. H. Lee, M. Lo Russo, J. Kim, M. Cammarata, Q. Kong, S. Noel, A. Plech, M. Wulff, H. Ihee, *Proc. Natl. Acad. Sci. USA* **2006**, *103*, 9410.
[16] Q. Y. Kong, M. Wulff, J. H. Lee, S. Bratos, H. Ihee, *J. Am. Chem. Soc.* **2007**, *129*, 13584.
[17] M. Wulff, S. Bratos, A. Plech, R. Vuilleumier, F. Mirloup, M. Lorenc, Q. Kong, H. Ihee, *J. Chem. Phys.* **2006**, *124*, 034501.
[18] M. Cammarata, M. Lorenc, T. K. Kim, J. H. Lee, Q. Y. Kong, E. Pontecorvo, M. Lo Russo, G. Schirò, A. Cupane, M. Wulff, H. Ihee, *J. Chem. Phys.* **2006**, *124*, 124504.
[19] E. Hunstock, C. Mealli, M. J. Calhorda, J. Reinhold, *Inorg. Chem.* **1999**, *38*, 5053.
[20] J. H. Lee, K. H. Kim, T. K. Kim, Y. Lee, H. Ihee, *J. Chem. Phys.* **2006**, *125*, 174504.
[21] J. Davidsson, J. Poulsen, M. Cammarata, P. Georgiou, R. Wouts, G. Katona, F. Jacobson, A. Plech, M. Wulff, G. Nyman, R. Neutze, *Phys. Rev. Lett.* **2005**, *94*, 245503.
[22] J. H. Lee, J. Kim, M. Cammarata, Q. Kong, K. H. Kim, J. Choi, T. K. Kim, M. Wulff, H. Ihee, *Angew. Chem.* **2008**, *120*, 1063; *Angew. Chem. Int. Ed.* **2008**, *47*, 1047.
[23] K. J. Gaffney, H. N. Chapman, *Science* **2007**, *316*, 1444.

